



CERN-EP-2016-177
LHCb-PAPER-2016-023
July 17, 2022

Search for the suppressed decays $B^+ \rightarrow K^+ K^+ \pi^-$ and $B^+ \rightarrow \pi^+ \pi^+ K^-$

The LHCb collaboration[†]

Abstract

A search is made for the highly-suppressed B meson decays $B^+ \rightarrow K^+ K^+ \pi^-$ and $B^+ \rightarrow \pi^+ \pi^+ K^-$ using a data sample corresponding to an integrated luminosity of 3.0 fb^{-1} collected by the LHCb experiment in proton-proton collisions at centre-of-mass energies of 7 and 8 TeV. No evidence is found for the decays, and upper limits at 90% confidence level are determined to be $\mathcal{B}(B^+ \rightarrow K^+ K^+ \pi^-) < 1.1 \times 10^{-8}$ and $\mathcal{B}(B^+ \rightarrow \pi^+ \pi^+ K^-) < 4.6 \times 10^{-8}$.

Submitted to Phys. Lett. B

© CERN on behalf of the LHCb collaboration, licence CC-BY-4.0.

[†]Authors are listed at the end of this paper.

1 Introduction

Transitions of the type $b \rightarrow ss\bar{d}$ and $b \rightarrow dd\bar{s}$ are rare in the Standard Model (SM) [1, 2]. The calculation of the $b \rightarrow ss\bar{d}$ amplitude results in branching fractions of at most $\mathcal{O}(10^{-11})$, the exact value depending on the unknown relative phase between t and c quark contributions in the W^\pm -exchange box [3], as shown in Fig. 1. The magnitude of the $b \rightarrow dd\bar{s}$ amplitude is expected to be even smaller due to the relative $|V_{td}/V_{ts}|$ factor, leading to predicted branching fractions of $\mathcal{O}(10^{-14})$ [4].

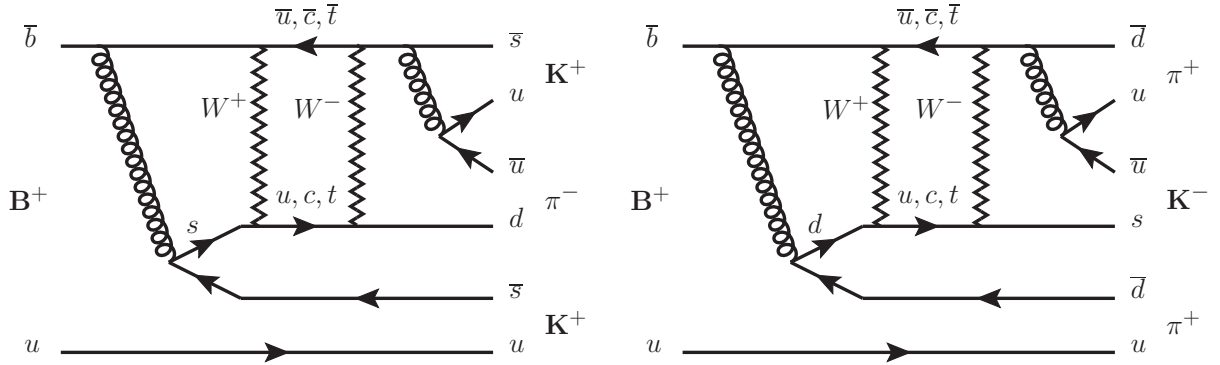


Figure 1: Main SM diagrams for the suppressed decays (left) $B^+ \rightarrow K^+ K^+ \pi^-$ and (right) $B^+ \rightarrow \pi^+ \pi^+ K^-$.

Physics beyond the Standard Model (BSM) could result in enhanced branching fractions that can be detected at current experiments. Theoretical models that have been investigated include the Minimal Supersymmetric Standard Model with and without R-Parity Violation, variations of the two Higgs doublet model, and extensions of the SM where an additional flavour changing Z' neutral boson is present [3, 4]. In these SM extensions, for certain plausible values of the model parameters, $b \rightarrow ss\bar{d}$ and $b \rightarrow dd\bar{s}$ transitions may lead to branching fractions of up to 10^{-8} and 10^{-7} , respectively. It has been suggested by these theoretical studies that the most suitable three-body decay modes to see the effects of BSM physics in such transitions are the $B^+ \rightarrow K^+ K^+ \pi^-$ and $B^+ \rightarrow \pi^+ \pi^+ K^-$ decays, where two particles in the final state have the same flavour and charge.¹

An upper limit of 1.29×10^{-4} at 90% confidence level on the branching fraction for the $B^+ \rightarrow \pi^+ \pi^+ K^-$ decay was first determined by OPAL [5]. Improvements in sensitivity were obtained by the e^+e^- B -factories, and currently the 90% confidence level upper limits for $B^+ \rightarrow K^+ K^+ \pi^-$ and $B^+ \rightarrow \pi^+ \pi^+ K^-$ decays are 1.6×10^{-7} and 9.5×10^{-7} , respectively [6–8].

This paper reports on the search for the suppressed decays $B^+ \rightarrow K^+ K^+ \pi^-$ and $B^+ \rightarrow \pi^+ \pi^+ K^-$ using data samples corresponding to 1.0 and 2.0 fb^{-1} collected by LHCb at $\sqrt{s} = 7$ and 8 TeV, respectively. The corresponding unsuppressed decays $B^+ \rightarrow K^+ K^- \pi^+$ and $B^+ \rightarrow \pi^+ \pi^- K^+$ are used for normalisation.

¹The inclusion of charge-conjugate decays is implied throughout.

2 Detector and simulation

The LHCb detector [9,10] is a single-arm forward spectrometer covering the pseudorapidity range $2 < \eta < 5$, designed for the study of particles containing b or c quarks. The detector includes a high-precision tracking system consisting of a silicon-strip vertex detector surrounding the pp interaction region, a large-area silicon-strip detector located upstream of a dipole magnet with a bending power of about 4 Tm, and three stations of silicon-strip detectors and straw drift tubes placed downstream of the magnet. The polarity of the dipole magnet is reversed periodically throughout data-taking. The configuration with the magnetic field vertically upwards (downwards) bends positively (negatively) charged particles in the horizontal plane towards the centre of the LHC. The tracking system provides a measurement of momentum, p , of charged particles with a relative uncertainty that varies from 0.5% at low momentum to 1.0% at 200 GeV/ c . The impact parameter (IP) is the minimum distance of a track to a primary vertex (PV) and is measured with a resolution of $(15 + 29/p_T) \mu\text{m}$, where p_T is the component of the momentum transverse to the beam, in GeV/ c . Different types of charged hadrons are distinguished using information from two ring-imaging Cherenkov detectors (RICH). Photons, electrons and hadrons are identified by a calorimeter system consisting of scintillating-pad and preshower detectors, an electromagnetic calorimeter and a hadronic calorimeter. Muons are identified by a system composed of alternating layers of iron and multiwire proportional chambers.

The online event selection is performed by a trigger [11], which consists of a hardware stage, based on information from the calorimeter and muon systems, followed by a software stage, which applies a full event reconstruction. At the hardware stage, the candidates are triggered either one of the particles from the b candidate decay depositing a transverse energy of at least 3500 MeV in the calorimeter, or by other activity in the event, mainly associated with the decay products of the other b hadron produced in the pp primary interaction.

Simulated $B^+ \rightarrow K^+ K^\pm \pi^\mp$ and $B^+ \rightarrow \pi^+ \pi^\pm K^\mp$ decays, generated uniformly in phase space, are used to optimize the suppressed signal selections and to evaluate the ratios of the efficiencies for each suppressed decay mode relative to their corresponding unsuppressed decay modes. In the simulation, pp collisions are generated using PYTHIA 8 [12, 13] with a specific LHCb configuration [14]. Decays of hadronic particles are described by EVTGEN [15] in which final state radiation is generated by PHOTOS [16]. The interaction of the generated particles with the detector and its response are implemented using the GEANT4 toolkit [17] as described in Ref. [18].

3 Event selection

The candidate $B^+ \rightarrow K^+ K^\pm \pi^\mp$ and $B^+ \rightarrow \pi^+ \pi^\pm K^\mp$ decays are reconstructed using three charged tracks with mass hypotheses and total charge consistent with the decay. The final state particles are required to have a good track fit with a reduced chi-square $\chi^2/\text{ndf} < 3$. All three tracks must have momentum $p > 1500 \text{ MeV}/c$, transverse momentum $p_T > 100 \text{ MeV}/c$, and $\chi_{\text{IP}}^2 > 1$ with respect to all PVs in the event. The quantity χ_{IP}^2 is defined as the difference between the vertex-fit χ^2 of the PV reconstructed with and without the considered track. Combinatorial backgrounds are suppressed by requiring that the scalar sum of the p_T of the tracks is greater than 4500 MeV/ c and the sum of the

tracks' $\chi_{\text{IP}}^2 > 200$. The track with the highest p_{T} must have $\text{IP} > 0.05$ mm. The second highest track p_{T} is required to be greater than 900 MeV/c. The maximum distance of closest approach between tracks has to be less than 0.2 mm.

The information from the RICH, the calorimeters and the muon systems is used for particle identification (PID) and requirements are applied to identify π and K tracks before forming a B^+ candidate. Muons are rejected by a veto applied to each track.

The reconstructed B^+ candidates are required to have an invariant mass in the range 5080 – 5480 MeV/c², $p_{\text{T}} > 1700$ MeV/c, $\chi_{\text{IP}}^2 < 10$, vertex fit $\chi^2/\text{ndf} < 12$, distance between the PV and the decay point (or secondary vertex, SV) greater than 3 mm, and a significant displacement between primary and secondary vertex, with the three dimensional χ^2 -distance between the two greater than 700. When more than one PV is reconstructed, the one with the minimum χ_{IP}^2 for the B^+ candidate is chosen. The cosine of the angle θ_f between the reconstructed momentum of the B^+ candidate and the B^+ candidate flight direction is required to be $\cos \theta_f > 0.99998$. The pointing variable $\theta_p \equiv P_B \sin \theta / (P_B \sin \theta + \sum_i^3 q_{\text{T}i})$ is required to be less than 0.05, where P_B is the total momentum of the three-particle final state, θ is the angle between the direction of the sum of the momenta of the charged tracks and the momentum direction of the B^+ candidate inferred from the PV and SV positions, and $\sum_i^3 q_{\text{T}i}$ is the sum of the transverse momenta of the three tracks with respect to the momentum direction of the B^+ candidate. These requirements remove additional combinatorial background and partially reconstructed b hadron decays. To avoid any artificial charge asymmetries in either signal or normalisation channels introduced by different acceptances while running with up and down magnet polarities, an additional criterion is placed on the x and z components² of the B^+ candidate momentum such that $|p_x| \leq 0.317 \times (p_z - 2400 \text{ MeV}/c)$ [19].

A B^+ candidate is rejected if the invariant mass formed from two of the charged tracks with opposite charge is within 25 MeV/c² of the D^0 mass. The D^0 veto suppresses possible background from $B^+ \rightarrow D^0 h^+$ decays. The $B^0 \rightarrow D^-(\rightarrow K^-\pi^+\pi^-)h^+$ background is found to be negligible. For $B^+ \rightarrow \pi^+\pi^-K^+$ decays only, an additional invariant mass criterion of $|3104 \text{ MeV}/c^2 - m_{\pi^+\pi^-}| > 20 \text{ MeV}/c^2$ is required to eliminate contamination $J/\psi \rightarrow \mu^+\mu^-$, where the muons are misidentified as pions, and from $J/\psi \rightarrow \pi^+\pi^-$.

The reconstructed candidates that meet the above criteria are filtered using a boosted decision tree (BDT) algorithm [20,21]. The BDT is trained with a sample of simulated signal candidates and a background sample of data candidates taken from the B^+ candidate invariant mass sideband above 5400 MeV/c², which is dominated by combinatorial background. The training is performed separately for events that have been triggered by information from the signal decay only and for events that have been triggered by other particles. This is required as the two trigger scenarios have different sensitivities to the signal and background. The input variables are chosen to produce the best discrimination and to minimise the dependence of the BDT on the mass of the B^+ candidate, the PID variables and on the kinematic configuration of the B^+ candidate parametrised in the Dalitz plane. The twelve variables used by the BDT are: the B^+ candidate p_{T} ; the flight distance between the PV and B^+ candidate SV; the angle θ_f ; the B^+ candidate pointing angle θ_p ; the p_{T} of the track with the lowest p_{T} ; the sum of the tracks' p_{T} ; the sum of the χ_{IP}^2 of the three tracks; the IP of the track with the highest p_{T} , with respect to the PV;

²In the LHCb right handed coordinate system, the z -axis points from the interaction point into the experiment and the y -axis is vertical, pointing upwards.

the momentum p of each of the three tracks; and the χ_{IP}^2 of the track reconstructed with the π hypothesis for $B^+ \rightarrow K^+ K^\pm \pi^\mp$ decays or the K hypothesis for $B^+ \rightarrow \pi^+ \pi^\pm K^\mp$ decays. The same set of variables is found to result in a robust multivariate classifier for the four decay channels under consideration.

A figure of merit $\text{FOM} \equiv \epsilon / (0.5 \times N_\sigma + \sqrt{N_B})$, is used to identify the optimal BDT selection criteria. Here ϵ is the simulated signal selection efficiency, N_B is the number of background events that pass the selection and have a mass in a $\pm 50 \text{ MeV}/c^2$ window around the B^\pm mass [22], and N_σ is the required significance, expressed in terms of standard deviations from the hypothesis of a null signal [23]. The quantity FOM is optimized with $N_\sigma = 5$, but the final result is robust against changes of one or two units in N_σ . For $B^+ \rightarrow K^+ K^+ \pi^-$, the optimal BDT selection criterion results in 85% of the simulated signal events being accepted and 71% of the background events rejected. For $B^+ \rightarrow \pi^+ \pi^+ K^-$, 67% of the simulated signal events are accepted and 91% of the background events are rejected.

The final selection is based on criteria applied to the probability for each of the three tracks to be a π or K . The same FOM optimisation described above is performed for each of the six probabilities in turn, starting with the track with the highest p_T . After application of these criteria, less than 2–4% of events have more than one candidate, depending on the decay mode. For these multiple candidate events, one candidate is chosen at random and the others discarded.

The efficiencies of all the selection requirements are calculated with simulated events. The PID efficiency for hadrons is determined from data using large calibration samples of $D^{*+} \rightarrow D^0(\rightarrow K^- \pi^+) \pi^+$ decays. The PID efficiencies in the simulated sample are corrected by reweighting the calibration sample to match the momentum and the pseudorapidity distributions of the final state particles in the signal decay and the multiplicity of tracks in the event.

After all selection criteria have been applied, the ratio of the $B^+ \rightarrow K^+ K^- \pi^+$ to $B^+ \rightarrow K^+ K^+ \pi^-$ selection efficiencies, weighted by the integrated luminosity taken with different magnet polarities and beam energy, is 1.00 ± 0.02 , while the ratio of the $B^+ \rightarrow \pi^+ \pi^- K^+$ to $B^+ \rightarrow \pi^+ \pi^+ K^-$ selection efficiencies is 0.97 ± 0.01 . The quoted uncertainties are statistical only and are due to the limited simulation sample size. The relative variation in the selection efficiency across the Dalitz plane is less than 8% for all four channels.

4 Determination of the signal yields

Signal yields are determined from simultaneous, unbinned and extended maximum likelihood fits to the invariant mass distributions $m_{h+h^\pm h'^\mp}$ of the suppressed and unsuppressed decays, where h and h' denote π or K . Separate fits are made for $B^+ \rightarrow K^+ K^+ \pi^-$ and $B^+ \rightarrow K^+ K^- \pi^+$ decays, and for $B^+ \rightarrow \pi^+ \pi^+ K^-$ and $B^+ \rightarrow \pi^+ \pi^- K^+$ decays.

The signal component for both the suppressed and unsuppressed decays is parameterised as the sum of a Gaussian function and a Crystal Ball function [24]. The values of the signal function parameters are constrained to be the same for both the suppressed and unsuppressed signal components.

For all decay modes, the combinatorial background is parameterised with an exponential function. Partially reconstructed backgrounds, largely due to B decays with four or more

particles in the final state, where one or more particles are not reconstructed, appear predominantly at $m_{h+h^\pm h'^\mp}$ masses below $5150 \text{ MeV}/c^2$ and are modelled with an ARGUS function [25] convolved with a Gaussian resolution function. In the case of the suppressed $B^+ \rightarrow \pi^+ \pi^+ K^-$ mode, an additional component, modelled in the same way, is used to account for B_s^0 four-body decays such as $B_s^0 \rightarrow D_s^- \pi^+$, with $D_s^- \rightarrow K^- \pi^+ \pi^-$, where one of the decay particles is not reconstructed. These appear at $m_{h+h^\pm h'^\mp}$ masses below $5250 \text{ MeV}/c^2$. The slope parameter of this ARGUS function is fixed from a fit to simulated decays. The signal yields, background yields, and all signal and background parameters (apart from the fixed slope parameter of the $B_s^0 \rightarrow D_s^- \pi^+$ component) are allowed to float in the fit.

To investigate the presence of any peaking background in the signal mass region, a large number of inclusive simulated B , B_s^0 , Λ_b^0 , and Ξ_b events are reconstructed using the same selection criteria used for the signal decay modes. The Dalitz plot distributions of the selected data, excluding the mass range $5230 < m_{h+h^\pm h'^\mp} < 5320 \text{ MeV}/c^2$, have also been studied to identify any resonances that might affect the determination of the signal yield. There is no evidence for any peaking background in the signal mass region.

The performance of the fit procedure is tested by creating ensembles of simulated datasets generated from the functions fitted to the data. A large number of datasets is generated and fits are performed with the number of signal and background events left free to fluctuate according to a Poisson distribution. The fit biases on the signal yields extracted from the pseudoexperiments are 0.05 ± 0.10 and -0.48 ± 0.15 events for the $B^+ \rightarrow K^+ K^+ \pi^-$ and $B^+ \rightarrow \pi^+ \pi^+ K^-$ decays, respectively, where the uncertainty is statistical only.

Figure 2 shows the fit to the $B^+ \rightarrow K^+ K^+ \pi^-$ and $B^+ \rightarrow K^+ K^- \pi^+$ decay candidates. The signal yields are -7.2 ± 4.6 and 955 ± 75 for $B^+ \rightarrow K^+ K^+ \pi^-$ and $B^+ \rightarrow K^+ K^- \pi^+$ respectively. Figure 3 shows the fit to the $B^+ \rightarrow \pi^+ \pi^+ K^-$ and $B^+ \rightarrow \pi^+ \pi^- K^+$ decay candidates. The signal yields are 2.7 ± 10.0 and 24044 ± 193 for $B^+ \rightarrow \pi^+ \pi^+ K^-$ and $B^+ \rightarrow \pi^+ \pi^- K^+$, respectively. The $B^+ \rightarrow K^+ K^+ \pi^-$ and $B^+ \rightarrow \pi^+ \pi^+ K^-$ signal yields have been corrected for the fit bias introduced by the fitting procedure.

The branching fractions of the suppressed decays are calculated using

$$\mathcal{B}_{\text{sup}} = \frac{N_{\text{sig}}^{\text{sup}}}{N_{\text{sig}}^{\text{unsup}}} \times \frac{\epsilon^{\text{unsup}}}{\epsilon^{\text{sup}}} \times \mathcal{B}_{\text{unsup}}, \quad (1)$$

where $N_{\text{sig}}^{\text{unsup}}$ and $N_{\text{sig}}^{\text{sup}}$ are the numbers of fitted signal events for the unsuppressed and suppressed modes (corrected for fit bias), while ϵ^{unsup} and ϵ^{sup} are the selection efficiencies calculated from simulated events and corrected for differences in selection efficiency between simulation and data. Finally, $\mathcal{B}_{\text{unsup}}$ is the known branching fraction for the unsuppressed reference mode [22].

5 Systematic uncertainties

The measurements of the branching fractions of the suppressed modes depend on the ratios of suppressed to unsuppressed signal yields and selection efficiencies. Since the final state is the same, apart from the charge assignment, the ratio of unsuppressed and suppressed selection efficiencies is close to unity, and most of the systematic uncertainties cancel.

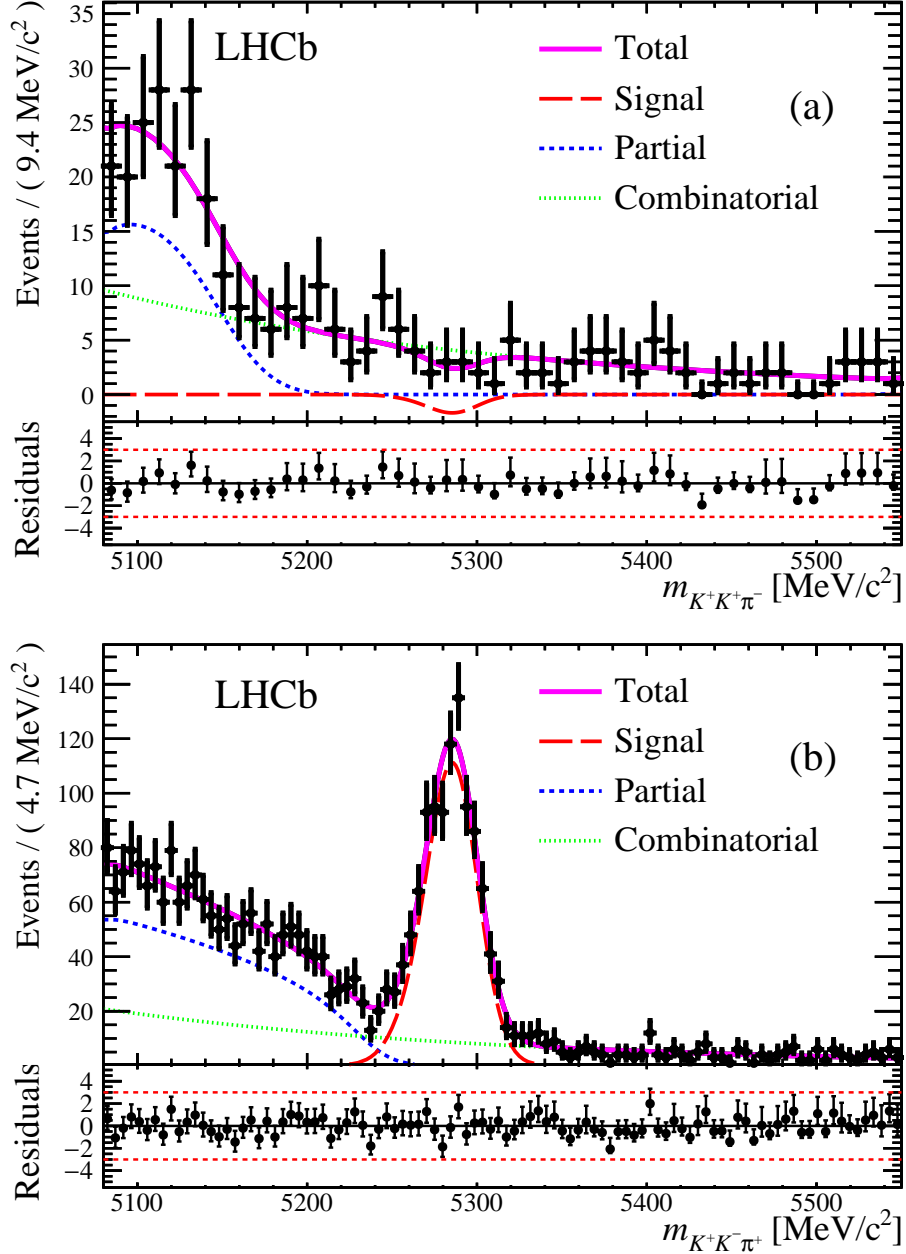


Figure 2: Invariant mass spectra of (a) $B^+ \rightarrow K^+ K^+ \pi^-$ and (b) $B^+ \rightarrow K^+ K^- \pi^+$ candidates, with the results of the unbinned extended maximum likelihood fits overlaid. The dashed (blue) line represents the partially reconstructed background, the dotted (green) line the combinatorial background, the long dashed (red) line is the signal, and the solid (magenta) line the total. Residual differences between data and the fits are shown below the mass plots in units of standard deviation.

The main systematic uncertainties on the branching fractions are due to the unsuppressed branching fraction uncertainties, PID charge dependence, discrepancies in PID between data and simulated events, fit biases, alternative mass fit models, simulated event statistics, and assumptions concerning the Dalitz plot distributions.

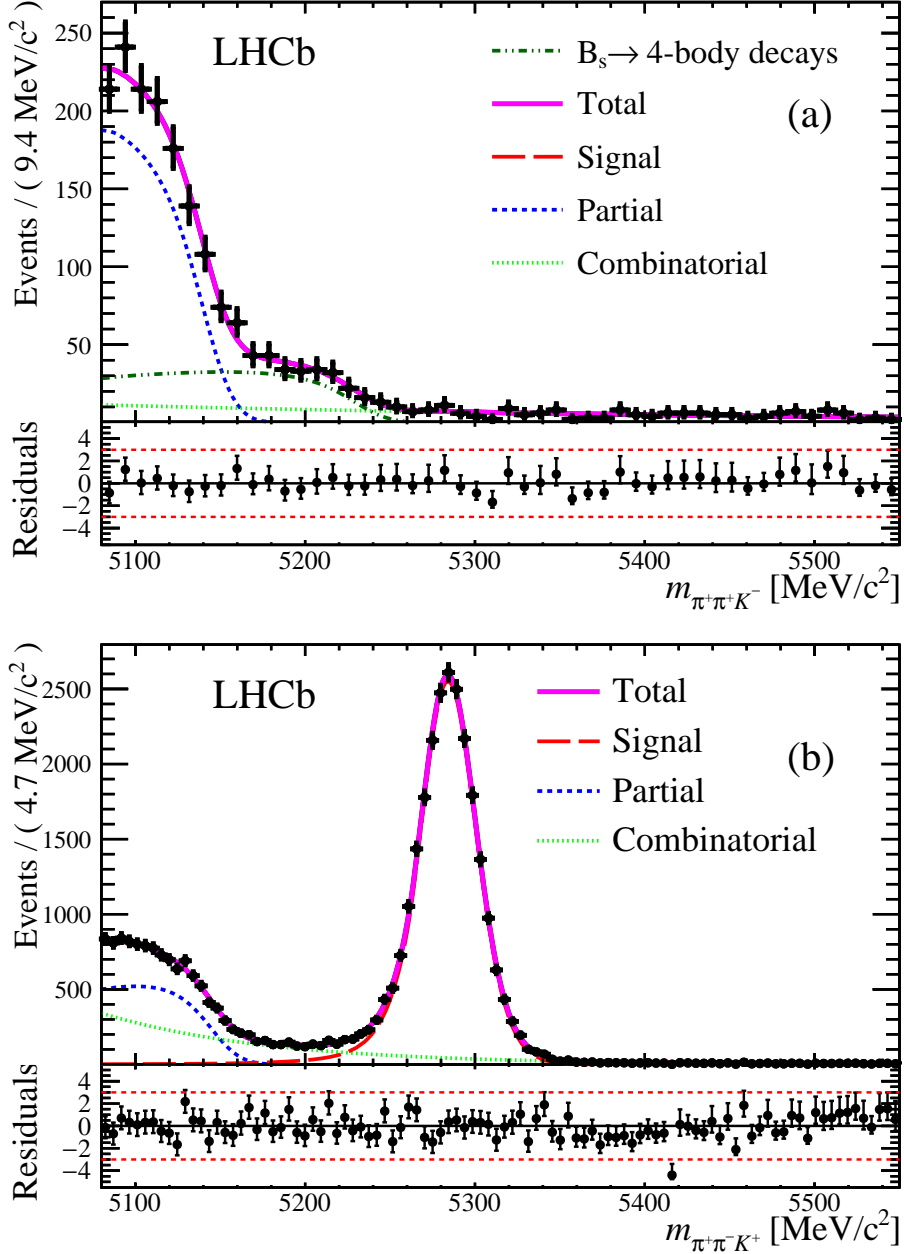


Figure 3: Invariant mass spectra of (a) $B^+ \rightarrow \pi^+\pi^+K^-$ and (b) $B^+ \rightarrow \pi^+\pi^-K^+$ candidates, with the results of the unbinned extended maximum likelihood fits overlaid. The dashed (blue) line represents the partially reconstructed background, the dotted (green) line the combinatorial background, the long dashed (red) line is the signal, the dot-dash (dark green) line the B_s^0 four-body backgrounds, and the solid (magenta) line the total. Residual differences between data and the fits are shown below the mass plots in units of standard deviation.

The uncertainties on the known $B^+ \rightarrow K^+K^-\pi^+$ and $B^+ \rightarrow \pi^+\pi^-K^+$ branching fractions result in systematic uncertainties of 0.53×10^{-8} and 0.32×10^{-9} , respectively [26–28]. Systematic uncertainties of 0.04×10^{-8} and 0.03×10^{-9} are assigned to the $B^+ \rightarrow K^+K^-\pi^+$ and $B^+ \rightarrow \pi^+\pi^-K^+$ decay modes, respectively, to account for the effect of

limited simulated events available to determine the reconstruction efficiencies.

Studies have shown a small PID dependence on the track charge with differences in efficiency below 0.2% for π^\pm and below 0.4% for K^\pm . Systematic uncertainties of 0.04×10^{-8} are assigned to both the $B^+ \rightarrow K^+ K^- \pi^+$ and the $B^+ \rightarrow \pi^+ \pi^- K^+$ branching fractions, derived from a 0.2% systematic uncertainty per pion and 0.4% per kaon, added linearly. The PID efficiency is extracted from data and systematic uncertainties of 0.09×10^{-8} and 0.11×10^{-9} are applied to $B^+ \rightarrow K^+ K^+ \pi^-$ and $B^+ \rightarrow \pi^+ \pi^+ K^-$, respectively, to account for different data-taking conditions.

To allow for possible differences in efficiency as a function of the Dalitz plot distributions, simulated events are generated with a distribution of resonances taken from previous published results, which are however only available for the $B^+ \rightarrow \pi^+ \pi^- K^+$ decay [26, 27]. There is an $(8 \pm 2)\%$ difference in the overall efficiency and this is taken as the maximum difference between a phase-space and a resonance-allowed distribution for all the modes. The resulting uncertainties are 0.15×10^{-8} and 0.22×10^{-9} for $B^+ \rightarrow K^+ K^+ \pi^-$ and $B^+ \rightarrow \pi^+ \pi^+ K^-$, respectively.

The fit bias from the ensemble of simulated pseudoexperiments generated from the fit to data is used to correct the signal yield observed in data. The systematic uncertainty on this correction is defined as half the fit bias added in quadrature with the fit bias statistical uncertainty. The systematic uncertainties introduced by this procedure are 0.05×10^{-8} and 0.58×10^{-9} for the $B^+ \rightarrow K^+ K^+ \pi^-$ and $B^+ \rightarrow \pi^+ \pi^+ K^-$ branching fractions, respectively.

To understand the impact of the fit model on the results, the components of the default models are changed independently. The signal component is replaced with a Crystal Ball function. The slope parameter of the $B_s^0 \rightarrow D_s^- \pi^+$ ARGUS function is allowed to float and the $B_s^0 \rightarrow D_s^- \pi^+$ component is replaced with a bifurcated Gaussian function. The combinatorial background distribution is modelled with a second order polynomial instead of an exponential. Studies of cross-feed from simulated unsuppressed $B^+ \rightarrow h^+ h^- h^+$ decays, where the flavour of one or more particles is misidentified, indicate 5.7 ± 2.7 events in the $B^+ \rightarrow K^+ K^+ \pi^-$ decay mode and 3.1 ± 1.8 events in $B^+ \rightarrow \pi^+ \pi^+ K^-$ decay mode. The uncertainty is dominated by limited simulation sample size. Cross-feed events are shifted by a minimum of $\sim 40 \text{ MeV}/c^2$ above and below the B mass. The fit is therefore repeated with two additional Gaussian functions centred around $5240 \text{ MeV}/c^2$ and $5320 \text{ MeV}/c^2$, respectively. As a cross-check, the fit is repeated with the means and widths of the Gaussian component allowed to vary. The fitted yields are compatible with zero. Systematic uncertainties of 0.45×10^{-8} and 0.29×10^{-9} are assigned for the $B^+ \rightarrow K^+ K^+ \pi^-$ and $B^+ \rightarrow \pi^+ \pi^+ K^-$ decays, respectively.

The total systematic uncertainty is determined by adding the individual contributions in quadrature. A summary of the systematic uncertainties is given in Table 1. The total systematic uncertainties are 0.72×10^{-8} and 0.76×10^{-9} for $B^+ \rightarrow K^+ K^+ \pi^-$ and $B^+ \rightarrow \pi^+ \pi^+ K^-$, respectively.

Table 1: Systematic uncertainties on the $B^+ \rightarrow K^+ K^+ \pi^-$ and $B^+ \rightarrow \pi^+ \pi^+ K^-$ branching fractions in units of 10^{-8} and 10^{-9} , respectively.

Criteria	$B^+ \rightarrow K^+ K^+ \pi^-$	$B^+ \rightarrow \pi^+ \pi^+ K^-$
Simulation statistics	0.04	0.03
PID charge dependence	0.04	0.04
PID discrepancies	0.09	0.11
Dalitz plot efficiencies	0.15	0.22
Fit bias	0.05	0.58
Fit model	0.45	0.29
Subtotal	0.49	0.69
PDG $\mathcal{B}_{\text{unsup}}$ uncertainty [22]	0.53	0.32
Total	0.72	0.76

6 Results and conclusions

Including all statistical and systematic uncertainties, the ratios of branching fractions are calculated to be

$$\begin{aligned} \frac{\mathcal{B}(B^+ \rightarrow K^+ K^+ \pi^-)}{\mathcal{B}(B^+ \rightarrow K^+ K^- \pi^+)} &= (-7.5 \pm 4.9 \pm 1.0) \times 10^{-3}, \\ \frac{\mathcal{B}(B^+ \rightarrow \pi^+ \pi^+ K^-)}{\mathcal{B}(B^+ \rightarrow \pi^+ \pi^- K^+)} &= (1.1 \pm 4.0 \pm 0.1) \times 10^{-4}, \end{aligned}$$

where the first uncertainties are statistical and the second are systematic. Using the above and the world average of the unsuppressed branching fractions [22] and using Eq. 1, we calculate the branching fractions

$$\begin{aligned} \mathcal{B}(B^+ \rightarrow K^+ K^+ \pi^-) &= (-3.8 \pm 2.4 \pm 0.5 \pm 0.5) \times 10^{-8}, \\ \mathcal{B}(B^+ \rightarrow \pi^+ \pi^+ K^-) &= (5.6 \pm 21.0 \pm 0.7 \pm 0.3) \times 10^{-9}, \end{aligned} \tag{2}$$

where the first uncertainties are statistical, the second are systematic without the unsuppressed decay branching fraction uncertainties, and the third are associated with the present knowledge of the $B^+ \rightarrow K^+ K^- \pi^+$ and $B^+ \rightarrow \pi^+ \pi^- K^+$ branching fractions.

To obtain upper limits on the branching fractions, the frequentist approach of Feldman and Cousins [29] is used to determine 90% and 95% confidence region bands that relate the true values of the branching fractions to the measured numbers of signal events. These bands are constructed using the results of simulation studies that account for relevant biases in the fit procedure and include statistical and systematic uncertainties. The construction of the confidence region bands is shown in Fig. 4. The 90% (95%) confidence level (CL) upper limits are found to be

$$\begin{aligned} \mathcal{B}(B^+ \rightarrow K^+ K^+ \pi^-) &< 1.1 \times 10^{-8} \text{ (} 1.8 \times 10^{-8} \text{) at 90\% (95\%) CL,} \\ \mathcal{B}(B^+ \rightarrow \pi^+ \pi^+ K^-) &< 4.6 \times 10^{-8} \text{ (} 5.7 \times 10^{-8} \text{) at 90\% (95\%) CL.} \end{aligned}$$

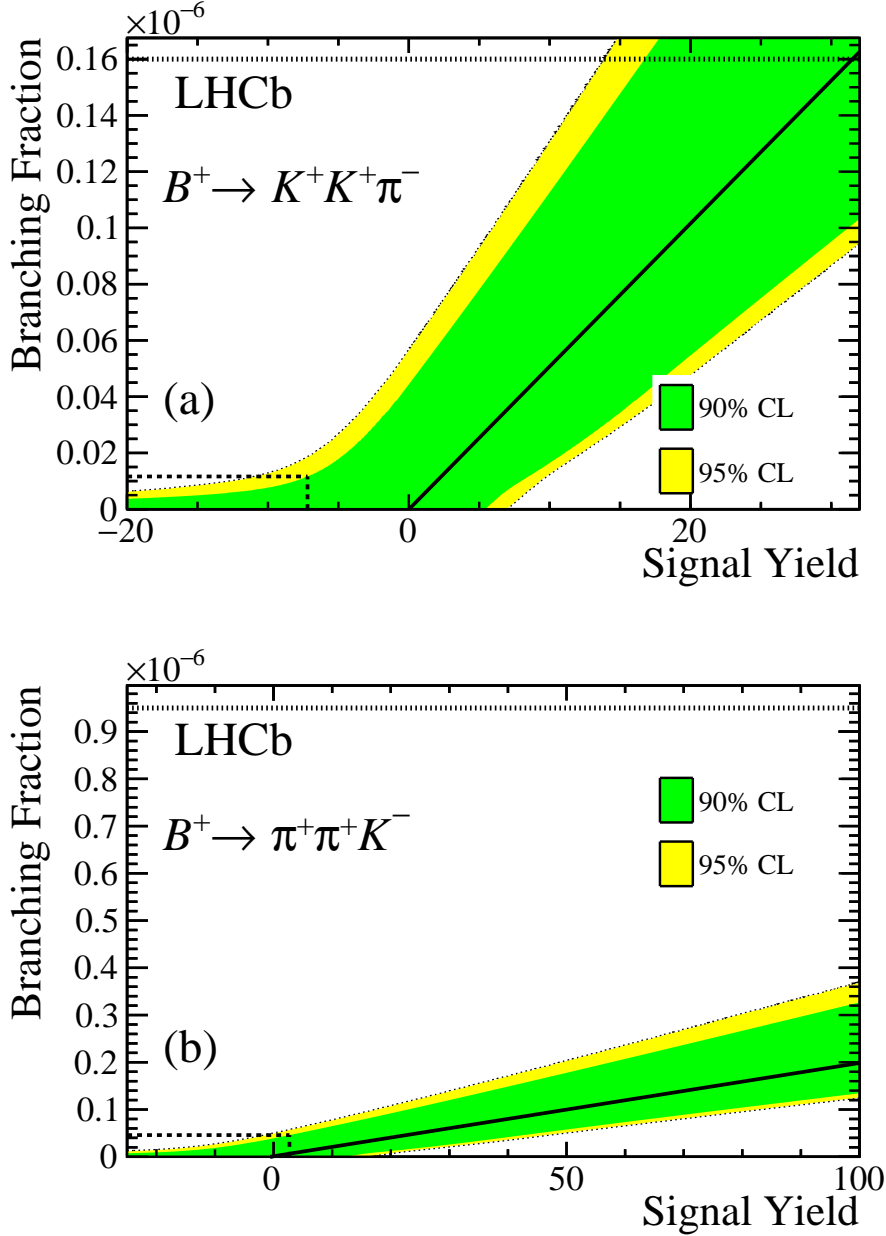


Figure 4: Feldman-Cousins 90% (green) and 95% (yellow) confidence level (CL) bands for (a) $B^+ \rightarrow K^+ K^+ \pi^-$ and (b) $B^+ \rightarrow \pi^+ \pi^+ K^-$, including statistical and systematic uncertainties. The black solid line shows the expected central value of the true branching fraction as a function of the fitted number of signal events. The horizontal dotted lines show the 90% CL upper limits on the branching fractions prior to the present measurement. The dashed lines in the lower left corner of each figure show the equivalent 90% CL upper limits reported in this paper.

In summary, searches are presented for the highly-suppressed decays $B^+ \rightarrow K^+ K^+ \pi^-$ and $B^+ \rightarrow \pi^+ \pi^+ K^-$ using a data sample of 3.0 fb^{-1} collected by the LHCb experiment in proton-proton collisions at the centre-of-mass energies of 7 and 8 TeV. No evidence is found for these decays and upper limits are placed on $B^+ \rightarrow K^+ K^+ \pi^-$ and $B^+ \rightarrow \pi^+ \pi^+ K^-$.

branching fractions. The results are approximately fourteen and twenty times more stringent, than previous measurements and constrain various extensions of the SM.

Acknowledgements

We express our gratitude to our colleagues in the CERN accelerator departments for the excellent performance of the LHC. We thank the technical and administrative staff at the LHCb institutes. We acknowledge support from CERN and from the national agencies: CAPES, CNPq, FAPERJ and FINEP (Brazil); NSFC (China); CNRS/IN2P3 (France); BMBF, DFG and MPG (Germany); INFN (Italy); FOM and NWO (The Netherlands); MNiSW and NCN (Poland); MEN/IFA (Romania); MinES and FANO (Russia); MinECo (Spain); SNSF and SER (Switzerland); NASU (Ukraine); STFC (United Kingdom); NSF (USA). We acknowledge the computing resources that are provided by CERN, IN2P3 (France), KIT and DESY (Germany), INFN (Italy), SURF (The Netherlands), PIC (Spain), GridPP (United Kingdom), RRCKI and Yandex LLC (Russia), CSCS (Switzerland), IFIN-HH (Romania), CBPF (Brazil), PL-GRID (Poland) and OSC (USA). We are indebted to the communities behind the multiple open source software packages on which we depend. Individual groups or members have received support from AvH Foundation (Germany), EPLANET, Marie Skłodowska-Curie Actions and ERC (European Union), Conseil Général de Haute-Savoie, Labex ENIGMASS and OCEVU, Région Auvergne (France), RFBR and Yandex LLC (Russia), GVA, XuntaGal and GENCAT (Spain), Herchel Smith Fund, The Royal Society, Royal Commission for the Exhibition of 1851 and the Leverhulme Trust (United Kingdom).

References

- [1] K. Huitu, D. X. Zhang, C. D. Lu, and P. Singer, *Searching for new physics in $b \rightarrow ss\bar{d}$ decays*, Phys. Rev. Lett. **81** (1998) 4313, [arXiv:hep-ph/9809566](#).
- [2] D. Pirjol and J. Zupan, *Predictions for $b \rightarrow ss\bar{d}$ and $b \rightarrow dd\bar{s}$ decays in the SM and with new physics*, JHEP **02** (2010) 028, [arXiv:0908.3150](#).
- [3] S. Fajfer and P. Singer, *Search for new physics in $\Delta S = 2$ two-body (VV , PP , VP) decays of the B^- meson*, Phys. Rev. **D62** (2000) 117702, [arXiv:hep-ph/0007132](#).
- [4] S. Fajfer, J. F. Kamenik, and N. Kosnik, *$b \rightarrow dd\bar{s}$ transition and constraints on new physics in B^- decays*, Phys. Rev. **D74** (2006) 034027, [arXiv:hep-ph/0605260](#).
- [5] OPAL collaboration, G. Abbiendi *et al.*, *Search for new physics in rare B decays*, Phys. Lett. **B476** (2000) 233, [arXiv:hep-ex/0002008](#).
- [6] Belle collaboration, K. Abe *et al.*, *Study of three-body charmless B decays*, Phys. Rev. **D65** (2002) 092005, [arXiv:hep-ex/0201007](#).
- [7] BaBar collaboration, B. Aubert *et al.*, *Measurements of the branching fractions and charge asymmetries of charmless three-body charged B decays*, Phys. Rev. Lett. **91** (2003) 051801, [arXiv:hep-ex/0304006](#).

- [8] BaBar collaboration, B. Aubert *et al.*, *Search for the highly suppressed decays $B^- \rightarrow K^+ \pi^- \pi^-$ and $B^- \rightarrow K^- K^- \pi^+$* , Phys. Rev. **D78** (2008) 091102, [arXiv:0808.0900](#).
- [9] LHCb collaboration, A. A. Alves Jr. *et al.*, *The LHCb detector at the LHC*, JINST **3** (2008) S08005.
- [10] LHCb collaboration, R. Aaij *et al.*, *LHCb detector performance*, Int. J. Mod. Phys. **A30** (2015) 1530022, [arXiv:1412.6352](#).
- [11] R. Aaij *et al.*, *The LHCb trigger and its performance in 2011*, JINST **8** (2013) P04022, [arXiv:1211.3055](#).
- [12] T. Sjöstrand, S. Mrenna, and P. Skands, *PYTHIA 6.4 physics and manual*, JHEP **05** (2006) 026, [arXiv:hep-ph/0603175](#).
- [13] T. Sjöstrand, S. Mrenna, and P. Skands, *A brief introduction to PYTHIA 8.1*, Comput. Phys. Commun. **178** (2008) 852, [arXiv:0710.3820](#).
- [14] I. Belyaev *et al.*, *Handling of the generation of primary events in Gauss, the LHCb simulation framework*, J. Phys. Conf. Ser. **331** (2011) 032047.
- [15] D. J. Lange, *The EvtGen particle decay simulation package*, Nucl. Instrum. Meth. **A462** (2001) 152.
- [16] P. Golonka and Z. Was, *PHOTOS Monte Carlo: A precision tool for QED corrections in Z and W decays*, Eur. Phys. J. **C45** (2006) 97, [arXiv:hep-ph/0506026](#).
- [17] Geant4 collaboration, J. Allison *et al.*, *Geant4 developments and applications*, IEEE Trans. Nucl. Sci. **53** (2006) 270.
- [18] M. Clemencic *et al.*, *The LHCb simulation application, Gauss: Design, evolution and experience*, J. Phys. Conf. Ser. **331** (2011) 032023.
- [19] H. Gordon, *Searches for CP violation in $D^+ \rightarrow K^- K^+ \pi^+$ decays at the LHCb experiment*, PhD thesis, Brasenose College, University of Oxford, 2013.
- [20] L. Breiman, J. H. Friedman, R. A. Olshen, and C. J. Stone, *Classification and regression trees*, Wadsworth international group, Belmont, California, USA, 1984.
- [21] R. E. Schapire and Y. Freund, *A decision-theoretic generalization of on-line learning and an application to boosting*, J. Comput. Syst. Sci. **55** (1997) 119.
- [22] Particle Data Group, K. A. Olive *et al.*, *Review of particle physics*, Chin. Phys. **C38** (2014) 090001, and 2015 update.
- [23] G. Punzi, *Sensitivity of searches for new signals and its optimization*, in *Statistical Problems in Particle Physics, Astrophysics, and Cosmology* (L. Lyons, R. Mount, and R. Reitmeyer, eds.), p. 79, 2003. [arXiv:physics/0308063](#).
- [24] T. Skwarnicki, *A study of the radiative cascade transitions between the Upsilon-prime and Upsilon resonances*, PhD thesis, Institute of Nuclear Physics, Krakow, 1986, DESY-F31-86-02.

- [25] ARGUS collaboration, H. Albrecht *et al.*, *Exclusive hadronic decays of B mesons*, Z. Phys. **C48** (1990) 543.
- [26] Belle collaboration, A. Garmash *et al.*, *Evidence for large direct CP violation in $B^\pm \rightarrow \rho(770)^0 K^\pm$ from analysis of the three-body charmless $B^\pm \rightarrow K^\pm \pi^\pm \pi^\mp$ decay*, Phys. Rev. Lett. **96** (2006) 251803, [arXiv:hep-ex/0512066](#).
- [27] BaBar collaboration, B. Aubert *et al.*, *Evidence for direct CP violation from Dalitz-plot analysis of $B^\pm \rightarrow K^\pm \pi^\mp \pi^\pm$* , Phys. Rev. **D78** (2008) 012004, [arXiv:0803.4451](#).
- [28] BaBar collaboration, B. Aubert *et al.*, *Observation of the decay $B^+ \rightarrow K^+ K^- \pi^+$* , Phys. Rev. Lett. **99** (2007) 221801, [arXiv:0708.0376](#).
- [29] G. J. Feldman and R. D. Cousins, *A unified approach to the classical statistical analysis of small signals*, Phys. Rev. **D57** (1998) 3873, [arXiv:physics/9711021](#).

LHCb collaboration

R. Aaij³⁹, B. Adeva³⁸, M. Adinolfi⁴⁷, Z. Ajaltouni⁵, S. Akar⁶, J. Albrecht¹⁰, F. Alessio³⁹, M. Alexander⁵², S. Ali⁴², G. Alkhazov³¹, P. Alvarez Cartelle⁵⁴, A.A. Alves Jr⁵⁸, S. Amato², S. Amerio²³, Y. Amhis⁷, L. An⁴⁰, L. Anderlini¹⁸, G. Andreassi⁴⁰, M. Andreotti^{17,g}, J.E. Andrews⁵⁹, R.B. Appleby⁵⁵, O. Aquines Gutierrez¹¹, F. Archilli¹, P. d'Argent¹², J. Arnau Romeu⁶, A. Artamonov³⁶, M. Artuso⁶⁰, E. Aslanides⁶, G. Auriemma^{26,s}, M. Baalouch⁵, I. Babuschkin⁵⁵, S. Bachmann¹², J.J. Back⁴⁹, A. Badalov³⁷, C. Baesso⁶¹, W. Baldini¹⁷, R.J. Barlow⁵⁵, C. Barschel³⁹, S. Barsuk⁷, W. Barter³⁹, V. Batozskaya²⁹, B. Batsukh⁶⁰, V. Battista⁴⁰, A. Bay⁴⁰, L. Beaucourt⁴, J. Beddow⁵², F. Bedeschi²⁴, I. Bediaga¹, L.J. Bel⁴², V. Bellee⁴⁰, N. Belloli^{21,i}, K. Belous³⁶, I. Belyaev³², E. Ben-Haim⁸, G. Bencivenni¹⁹, S. Benson³⁹, J. Benton⁴⁷, A. Berezhnoy³³, R. Bernet⁴¹, A. Bertolin²³, F. Betti¹⁵, M.-O. Bettler³⁹, M. van Beuzekom⁴², S. Bifani⁴⁶, P. Billoir⁸, T. Bird⁵⁵, A. Birnkraut¹⁰, A. Bitadze⁵⁵, A. Bizzeti^{18,u}, T. Blake⁴⁹, F. Blanc⁴⁰, J. Blouw¹¹, S. Blusk⁶⁰, V. Bocci²⁶, T. Boettcher⁵⁷, A. Bondar³⁵, N. Bondar^{31,39}, W. Bonivento¹⁶, A. Borgheresi^{21,i}, S. Borghi⁵⁵, M. Borisyak⁶⁷, M. Borsato³⁸, F. Bossu⁷, M. Boubdir⁹, T.J.V. Bowcock⁵³, E. Bowen⁴¹, C. Bozzi^{17,39}, S. Braun¹², M. Britsch¹², T. Britton⁶⁰, J. Brodzicka⁵⁵, E. Buchanan⁴⁷, C. Burr⁵⁵, A. Bursche², J. Buytaert³⁹, S. Cadeddu¹⁶, R. Calabrese^{17,g}, M. Calvi^{21,i}, M. Calvo Gomez^{37,m}, A. Camboni³⁷, P. Campana¹⁹, D. Campora Perez³⁹, D.H. Campora Perez³⁹, L. Capriotti⁵⁵, A. Carbone^{15,e}, G. Carboni^{25,j}, R. Cardinale^{20,h}, A. Cardini¹⁶, P. Carniti^{21,i}, L. Carson⁵¹, K. Carvalho Akiba², G. Casse⁵³, L. Cassina^{21,i}, L. Castillo Garcia⁴⁰, M. Cattaneo³⁹, Ch. Cauet¹⁰, G. Cavallero²⁰, R. Cenci^{24,t}, M. Charles⁸, Ph. Charpentier³⁹, G. Chatzikonstantinidis⁴⁶, M. Chefdeville⁴, S. Chen⁵⁵, S.-F. Cheung⁵⁶, V. Chobanova³⁸, M. Chrzaszcz^{41,27}, X. Cid Vidal³⁸, G. Ciezarek⁴², P.E.L. Clarke⁵¹, M. Clemencic³⁹, H.V. Cliff⁴⁸, J. Closier³⁹, V. Coco⁵⁸, J. Cogan⁶, E. Cogneras⁵, V. Cogoni^{16,f}, L. Cojocariu³⁰, G. Collazuol^{23,o}, P. Collins³⁹, A. Comerma-Montells¹², A. Contu³⁹, A. Cook⁴⁷, S. Coquereau⁸, G. Corti³⁹, M. Corvo^{17,g}, C.M. Costa Sobral⁴⁹, B. Couturier³⁹, G.A. Cowan⁵¹, D.C. Craik⁵¹, A. Crocombe⁴⁹, M. Cruz Torres⁶¹, S. Cunliffe⁵⁴, R. Currie⁵⁴, C. D'Ambrosio³⁹, E. Dall'Occo⁴², J. Dalseno⁴⁷, P.N.Y. David⁴², A. Davis⁵⁸, O. De Aguiar Francisco², K. De Bruyn⁶, S. De Capua⁵⁵, M. De Cian¹², J.M. De Miranda¹, L. De Paula², M. De Serio^{14,d}, P. De Simone¹⁹, C.-T. Dean⁵², D. Decamp⁴, M. Deckenhoff¹⁰, L. Del Buono⁸, M. Demmer¹⁰, D. Derkach⁶⁷, O. Deschamps⁵, F. Dettori³⁹, B. Dey²², A. Di Canto³⁹, H. Dijkstra³⁹, F. Dordei³⁹, M. Dorigo⁴⁰, A. Dosil Suárez³⁸, A. Dovbnya⁴⁴, K. Dreimanis⁵³, L. Dufour⁴², G. Dujany⁵⁵, K. Dungs³⁹, P. Durante³⁹, R. Dzhelezhyan³⁶, A. Dziurda³⁹, A. Dzyuba³¹, N. Deléage⁴, S. Easo⁵⁰, M. Ebert⁵¹, U. Egede⁵⁴, V. Egorychev³², S. Eidelman³⁵, S. Eisenhardt⁵¹, U. Eitschberger¹⁰, R. Ekelhof¹⁰, L. Eklund⁵², Ch. Elsasser⁴¹, S. Ely⁶⁰, S. Esen¹², H.M. Evans⁴⁸, T. Evans⁵⁶, A. Falabella¹⁵, N. Farley⁴⁶, S. Farry⁵³, R. Fay⁵³, D. Fazzini^{21,i}, D. Ferguson⁵¹, V. Fernandez Albor³⁸, A. Fernandez Prieto³⁸, F. Ferrari^{15,39}, F. Ferreira Rodrigues¹, M. Ferro-Luzzi³⁹, S. Filippov³⁴, M. Fiore^{17,g}, M. Fiorini^{17,g}, M. Firlej²⁸, C. Fitzpatrick⁴⁰, T. Fiutowski²⁸, F. Fleuret^{7,b}, K. Fohl³⁹, M. Fontana¹⁶, F. Fontanelli^{20,h}, D.C. Forshaw⁶⁰, R. Forty³⁹, M. Frank³⁹, C. Frei³⁹, J. Fu^{22,q}, E. Furfaro^{25,j}, C. Färber³⁹, A. Gallas Torreira³⁸, D. Galli^{15,e}, S. Gallorini²³, S. Gambetta⁵¹, M. Gandelman², P. Gandini⁵⁶, Y. Gao³, L.M. Garcia Martin⁶⁸, J. García Pardiñas³⁸, J. Garra Tico⁴⁸, L. Garrido³⁷, P.J. Garsed⁴⁸, D. Gascon³⁷, C. Gaspar³⁹, L. Gavardi¹⁰, G. Gazzoni⁵, D. Gerick¹², E. Gersabeck¹², M. Gersabeck⁵⁵, T. Gershon⁴⁹, Ph. Ghez⁴, S. Gianì⁴⁰, V. Gibson⁴⁸, O.G. Girard⁴⁰, L. Giubega³⁰, K. Gizdov⁵¹, V.V. Gligorov⁸, D. Golubkov³², A. Golutvin^{54,39}, A. Gomes^{1,a}, I.V. Gorelov³³, C. Gotti^{21,i}, M. Grabalosa Gándara⁵, R. Graciani Diaz³⁷, L.A. Granado Cardoso³⁹, E. Graugés³⁷, E. Graverini⁴¹, G. Graziani¹⁸, A. Greco³⁰, P. Griffith⁴⁶, L. Grillo¹², B.R. Gruber Cazon⁵⁶, O. Grünberg⁶⁵, E. Gushchin³⁴, Yu. Guz³⁶, T. Gys³⁹, C. Göbel⁶¹, T. Hadavizadeh⁵⁶, C. Hadjivasiliou⁶⁰, G. Haefeli⁴⁰, C. Haen³⁹, S.C. Haines⁴⁸,

S. Hall⁵⁴, B. Hamilton⁵⁹, X. Han¹², S. Hansmann-Menzemer¹², N. Harnew⁵⁶, S.T. Harnew⁴⁷,
 J. Harrison⁵⁵, M. Hatch³⁹, J. He⁶², T. Head⁴⁰, A. Heister⁹, K. Hennessy⁵³, P. Henrard⁵,
 L. Henry⁸, J.A. Hernando Morata³⁸, E. van Herwijnen³⁹, M. Heß⁶⁵, A. Hicheur², D. Hill⁵⁶,
 C. Hombach⁵⁵, W. Hulsbergen⁴², T. Humair⁵⁴, M. Hushchyn⁶⁷, N. Hussain⁵⁶, D. Hutchcroft⁵³,
 M. Idzik²⁸, P. Ilten⁵⁷, R. Jacobsson³⁹, A. Jaeger¹², J. Jalocha⁵⁶, E. Jans⁴², A. Jawahery⁵⁹,
 M. John⁵⁶, D. Johnson³⁹, C.R. Jones⁴⁸, C. Joram³⁹, B. Jost³⁹, N. Jurik⁶⁰, S. Kandybei⁴⁴,
 W. Kalso⁶, M. Karacson³⁹, J.M. Kariuki⁴⁷, S. Karodia⁵², M. Kecke¹², M. Kelsey⁶⁰,
 I.R. Kenyon⁴⁶, M. Kenzie³⁹, T. Ketel⁴³, E. Khairullin⁶⁷, B. Khanji^{21,39,i}, C. Khurewathanakul⁴⁰,
 T. Kirn⁹, S. Klaver⁵⁵, K. Klimaszewski²⁹, S. Koliiev⁴⁵, M. Kolpin¹², I. Komarov⁴⁰,
 R.F. Koopman⁴³, P. Koppenburg⁴², A. Kozachuk³³, M. Kozeiha⁵, L. Kravchuk³⁴, K. Kreplin¹²,
 M. Kreps⁴⁹, P. Krokovny³⁵, F. Kruse¹⁰, W. Krzemien²⁹, W. Kucewicz^{27,l}, M. Kucharczyk²⁷,
 V. Kudryavtsev³⁵, A.K. Kuonen⁴⁰, K. Kurek²⁹, T. Kvaratskheliya^{32,39}, D. Lacarrere³⁹,
 G. Lafferty^{55,39}, A. Lai¹⁶, D. Lambert⁵¹, G. Lanfranchi¹⁹, C. Langenbruch⁹, B. Langhans³⁹,
 T. Latham⁴⁹, C. Lazzeroni⁴⁶, R. Le Gac⁶, J. van Leerdam⁴², J.-P. Lees⁴, A. Leflat^{33,39},
 J. Lefrançois⁷, R. Lefèvre⁵, F. Lemaitre³⁹, E. Lemos Cid³⁸, O. Leroy⁶, T. Lesiak²⁷,
 B. Leverington¹², Y. Li⁷, T. Likhomanenko^{67,66}, R. Lindner³⁹, C. Linn³⁹, F. Lionetto⁴¹,
 B. Liu¹⁶, X. Liu³, D. Loh⁴⁹, I. Longstaff⁵², J.H. Lopes², D. Lucchesi^{23,o}, M. Lucio Martinez³⁸,
 H. Luo⁵¹, A. Lupato²³, E. Luppi^{17,g}, O. Lupton⁵⁶, A. Lusiani²⁴, X. Lyu⁶², F. Machefert⁷,
 F. Maciuc³⁰, O. Maev³¹, K. Maguire⁵⁵, S. Malde⁵⁶, A. Malinin⁶⁶, T. Maltsev³⁵, G. Manca⁷,
 G. Mancinelli⁶, P. Manning⁶⁰, J. Maratas⁵, J.F. Marchand⁴, U. Marconi¹⁵, C. Marin Benito³⁷,
 P. Marino^{24,t}, J. Marks¹², G. Martellotti²⁶, M. Martin⁶, M. Martinelli⁴⁰, D. Martinez Santos³⁸,
 F. Martinez Vidal⁶⁸, D. Martins Tostes², L.M. Massacrier⁷, A. Massafferri¹, R. Matev³⁹,
 A. Mathad⁴⁹, Z. Mathe³⁹, C. Matteuzzi²¹, A. Mauri⁴¹, B. Maurin⁴⁰, A. Mazurov⁴⁶,
 M. McCann⁵⁴, J. McCarthy⁴⁶, A. McNab⁵⁵, R. McNulty¹³, B. Meadows⁵⁸, F. Meier¹⁰,
 M. Meissner¹², D. Melnychuk²⁹, M. Merk⁴², A. Merli^{22,q}, E. Michielin²³, D.A. Milanes⁶⁴,
 M.-N. Minard⁴, D.S. Mitzel¹², J. Molina Rodriguez⁶¹, I.A. Monroy⁶⁴, S. Monteil⁵,
 M. Morandin²³, P. Morawski²⁸, A. Mordà⁶, M.J. Morello^{24,t}, J. Moron²⁸, A.B. Morris⁵¹,
 R. Mountain⁶⁰, F. Muheim⁵¹, M. Mulder⁴², M. Mussini¹⁵, D. Müller⁵⁵, J. Müller¹⁰, K. Müller⁴¹,
 V. Müller¹⁰, P. Naik⁴⁷, T. Nakada⁴⁰, R. Nandakumar⁵⁰, A. Nandi⁵⁶, I. Nasteva²,
 M. Needham⁵¹, N. Neri²², S. Neubert¹², N. Neufeld³⁹, M. Neuner¹², A.D. Nguyen⁴⁰,
 C. Nguyen-Mau^{40,n}, S. Nieswand⁹, R. Niet¹⁰, N. Nikitin³³, T. Nikodem¹², A. Novoselov³⁶,
 D.P. O'Hanlon⁴⁹, A. Oblakowska-Mucha²⁸, V. Obraztsov³⁶, S. Ogilvy¹⁹, R. Oldeman⁴⁸,
 C.J.G. Onderwater⁶⁹, J.M. Otalora Goicochea², A. Otto³⁹, P. Owen⁴¹, A. Oyanguren⁶⁸,
 P.R. Pais⁴⁰, A. Palano^{14,d}, F. Palombo^{22,q}, M. Palutan¹⁹, J. Panman³⁹, A. Papanestis⁵⁰,
 M. Pappagallo⁵², L.L. Pappalardo^{17,g}, C. Pappenheimer⁵⁸, W. Parker⁵⁹, C. Parkes⁵⁵,
 G. Passaleva¹⁸, G.D. Patel⁵³, M. Patel⁵⁴, C. Patrignani^{15,e}, A. Pearce^{55,50}, A. Pellegrino⁴²,
 G. Penso^{26,k}, M. Pepe Altarelli³⁹, S. Perazzini³⁹, P. Perret⁵, L. Pescatore⁴⁶, K. Petridis⁴⁷,
 A. Petrolini^{20,h}, A. Petrov⁶⁶, M. Petruzzo^{22,q}, E. Picatoste Olloqui³⁷, B. Pietrzyk⁴, M. Pikies²⁷,
 D. Pinci²⁶, A. Pistone²⁰, A. Piucci¹², S. Playfer⁵¹, M. Plo Casasus³⁸, T. Poikela³⁹, F. Polci⁸,
 A. Poluektov^{49,35}, I. Polyakov³², E. Polcarpo², G.J. Pomery⁴⁷, A. Popov³⁶, D. Popov^{11,39},
 B. Popovici³⁰, C. Potterat², E. Price⁴⁷, J.D. Price⁵³, J. Prisciandaro³⁸, A. Pritchard⁵³,
 C. Prouve⁴⁷, V. Pugatch⁴⁵, A. Puig Navarro⁴⁰, G. Punzi^{24,p}, W. Qian⁵⁶, R. Quagliani^{7,47},
 B. Rachwal²⁷, J.H. Rademacker⁴⁷, M. Rama²⁴, M. Ramos Pernas³⁸, M.S. Rangel², I. Raniuk⁴⁴,
 G. Raven⁴³, F. Redi⁵⁴, S. Reichert¹⁰, A.C. dos Reis¹, C. Remon Alepuz⁶⁸, V. Renaudin⁷,
 S. Ricciardi⁵⁰, S. Richards⁴⁷, M. Rühl³⁹, K. Rinnert^{53,39}, V. Rives Molina³⁷, P. Robbe^{7,39},
 A.B. Rodrigues¹, E. Rodrigues⁵⁸, J.A. Rodriguez Lopez⁶⁴, P. Rodriguez Perez⁵⁵,
 A. Rogozhnikov⁶⁷, S. Roiser³⁹, V. Romanovskiy³⁶, A. Romero Vidal³⁸, J.W. Ronayne¹³,
 M. Rotondo²³, T. Ruf³⁹, P. Ruiz Valls⁶⁸, J.J. Saborido Silva³⁸, E. Sadykhov³², N. Sagidova³¹,
 B. Saitta^{16,f}, V. Salustino Guimaraes², C. Sanchez Mayordomo⁶⁸, B. Sanmartin Sedes³⁸,
 R. Santacesaria²⁶, C. Santamarina Rios³⁸, M. Santimaria¹⁹, E. Santovetti^{25,j}, A. Sarti^{19,k},

C. Satriano^{26,s}, A. Satta²⁵, D.M. Saunders⁴⁷, D. Savrina^{32,33}, S. Schael⁹, M. Schiller³⁹, H. Schindler³⁹, M. Schlupp¹⁰, M. Schmelling¹¹, T. Schmelzer¹⁰, B. Schmidt³⁹, O. Schneider⁴⁰, A. Schopper³⁹, M. Schubiger⁴⁰, M.-H. Schune⁷, R. Schwemmer³⁹, B. Sciascia¹⁹, A. Sciubba^{26,k}, A. Semennikov³², A. Sergi⁴⁶, N. Serra⁴¹, J. Serrano⁶, L. Sestini²³, P. Seyfert²¹, M. Shapkin³⁶, I. Shapoval^{17,44,g}, Y. Shcheglov³¹, T. Shears⁵³, L. Shekhtman³⁵, V. Shevchenko⁶⁶, A. Shires¹⁰, B.G. Siddi¹⁷, R. Silva Coutinho⁴¹, L. Silva de Oliveira², G. Simi^{23,o}, S. Simone^{14,d}, M. Sirendi⁴⁸, N. Skidmore⁴⁷, T. Skwarnicki⁶⁰, E. Smith⁵⁴, I.T. Smith⁵¹, J. Smith⁴⁸, M. Smith⁵⁵, H. Snoek⁴², M.D. Sokoloff⁵⁸, F.J.P. Soler⁵², D. Souza⁴⁷, B. Souza De Paula², B. Spaan¹⁰, P. Spradlin⁵², S. Sridharan³⁹, F. Stagni³⁹, M. Stahl¹², S. Stahl³⁹, P. Steffen⁴⁰, S. Stefkova⁵⁴, O. Steinkamp⁴¹, O. Stenyakin³⁶, S. Stevenson⁵⁶, S. Stoica³⁰, S. Stone⁶⁰, B. Storaci⁴¹, S. Stracka^{24,t}, M. Straticiu³⁰, U. Straumann⁴¹, L. Sun⁵⁸, W. Sutcliffe⁵⁴, K. Swientek²⁸, V. Syropoulos⁴³, M. Szczekowski²⁹, T. Szumlak²⁸, S. T'Jampens⁴, A. Tayduganov⁶, T. Tekampe¹⁰, G. Tellarini^{17,g}, F. Teubert³⁹, C. Thomas⁵⁶, E. Thomas³⁹, J. van Tilburg⁴², V. Tisserand⁴, M. Tobin⁴⁰, S. Tolk⁴⁸, L. Tomassetti^{17,g}, D. Tonelli³⁹, S. Topp-Joergensen⁵⁶, F. Toriello⁶⁰, E. Tournefier⁴, S. Tourneur⁴⁰, K. Trabelsi⁴⁰, M. Traill⁵², M.T. Tran⁴⁰, M. Tresch⁴¹, A. Trisovic³⁹, A. Tsaregorodtsev⁶, P. Tsopelas⁴², A. Tully⁴⁸, N. Tuning⁴², A. Ukleja²⁹, A. Ustyuzhanin^{67,66}, U. Uwer¹², C. Vacca^{16,39,f}, V. Vagnoni^{15,39}, S. Valat³⁹, G. Valenti¹⁵, A. Vallier⁷, R. Vazquez Gomez¹⁹, P. Vazquez Regueiro³⁸, S. Vecchi¹⁷, M. van Veghel⁴², J.J. Velthuis⁴⁷, M. Veltri^{18,r}, G. Veneziano⁴⁰, A. Venkateswaran⁶⁰, M. Vesterinen¹², B. Viaud⁷, D. Vieira¹, M. Vieites Diaz³⁸, X. Vilasis-Cardona^{37,m}, V. Volkov³³, A. Vollhardt⁴¹, B. Voneki³⁹, D. Voong⁴⁷, A. Vorobyev³¹, V. Vorobyev³⁵, C. Voß⁶⁵, J.A. de Vries⁴², C. Vázquez Sierra³⁸, R. Waldi⁶⁵, C. Wallace⁴⁹, R. Wallace¹³, J. Walsh²⁴, J. Wang⁶⁰, D.R. Ward⁴⁸, H.M. Wark⁵³, N.K. Watson⁴⁶, D. Websdale⁵⁴, A. Weiden⁴¹, M. Whitehead³⁹, J. Wicht⁴⁹, G. Wilkinson^{56,39}, M. Wilkinson⁶⁰, M. Williams³⁹, M.P. Williams⁴⁶, M. Williams⁵⁷, T. Williams⁴⁶, F.F. Wilson⁵⁰, J. Kimberley⁵⁹, J. Wishahi¹⁰, W. Wislicki²⁹, M. Witek²⁷, G. Wormser⁷, S.A. Wotton⁴⁸, K. Wraight⁵², S. Wright⁴⁸, K. Wyllie³⁹, Y. Xie⁶³, Z. Xing⁶⁰, Z. Xu⁴⁰, Z. Yang³, H. Yin⁶³, J. Yu⁶³, X. Yuan³⁵, O. Yushchenko³⁶, M. Zangoli¹⁵, K.A. Zarebski⁴⁶, M. Zavertyaev^{11,c}, L. Zhang³, Y. Zhang⁷, Y. Zhang⁶², A. Zhelezov¹², Y. Zheng⁶², A. Zhokhov³², X. Zhu³, V. Zhukov⁹, S. Zucchelli¹⁵.

¹Centro Brasileiro de Pesquisas Físicas (CBPF), Rio de Janeiro, Brazil

²Universidade Federal do Rio de Janeiro (UFRJ), Rio de Janeiro, Brazil

³Center for High Energy Physics, Tsinghua University, Beijing, China

⁴LAPP, Université Savoie Mont-Blanc, CNRS/IN2P3, Annecy-Le-Vieux, France

⁵Clermont Université, Université Blaise Pascal, CNRS/IN2P3, LPC, Clermont-Ferrand, France

⁶CPPM, Aix-Marseille Université, CNRS/IN2P3, Marseille, France

⁷LAL, Université Paris-Sud, CNRS/IN2P3, Orsay, France

⁸LPNHE, Université Pierre et Marie Curie, Université Paris Diderot, CNRS/IN2P3, Paris, France

⁹I. Physikalisches Institut, RWTH Aachen University, Aachen, Germany

¹⁰Fakultät Physik, Technische Universität Dortmund, Dortmund, Germany

¹¹Max-Planck-Institut für Kernphysik (MPIK), Heidelberg, Germany

¹²Physikalisches Institut, Ruprecht-Karls-Universität Heidelberg, Heidelberg, Germany

¹³School of Physics, University College Dublin, Dublin, Ireland

¹⁴Sezione INFN di Bari, Bari, Italy

¹⁵Sezione INFN di Bologna, Bologna, Italy

¹⁶Sezione INFN di Cagliari, Cagliari, Italy

¹⁷Sezione INFN di Ferrara, Ferrara, Italy

¹⁸Sezione INFN di Firenze, Firenze, Italy

¹⁹Laboratori Nazionali dell'INFN di Frascati, Frascati, Italy

²⁰Sezione INFN di Genova, Genova, Italy

²¹Sezione INFN di Milano Bicocca, Milano, Italy

²²Sezione INFN di Milano, Milano, Italy

²³Sezione INFN di Padova, Padova, Italy

- ²⁴ *Sezione INFN di Pisa, Pisa, Italy*
- ²⁵ *Sezione INFN di Roma Tor Vergata, Roma, Italy*
- ²⁶ *Sezione INFN di Roma La Sapienza, Roma, Italy*
- ²⁷ *Henryk Niewodniczanski Institute of Nuclear Physics Polish Academy of Sciences, Kraków, Poland*
- ²⁸ *AGH - University of Science and Technology, Faculty of Physics and Applied Computer Science, Kraków, Poland*
- ²⁹ *National Center for Nuclear Research (NCBJ), Warsaw, Poland*
- ³⁰ *Horia Hulubei National Institute of Physics and Nuclear Engineering, Bucharest-Magurele, Romania*
- ³¹ *Petersburg Nuclear Physics Institute (PNPI), Gatchina, Russia*
- ³² *Institute of Theoretical and Experimental Physics (ITEP), Moscow, Russia*
- ³³ *Institute of Nuclear Physics, Moscow State University (SINP MSU), Moscow, Russia*
- ³⁴ *Institute for Nuclear Research of the Russian Academy of Sciences (INR RAN), Moscow, Russia*
- ³⁵ *Budker Institute of Nuclear Physics (SB RAS) and Novosibirsk State University, Novosibirsk, Russia*
- ³⁶ *Institute for High Energy Physics (IHEP), Protvino, Russia*
- ³⁷ *Universitat de Barcelona, Barcelona, Spain*
- ³⁸ *Universidad de Santiago de Compostela, Santiago de Compostela, Spain*
- ³⁹ *European Organization for Nuclear Research (CERN), Geneva, Switzerland*
- ⁴⁰ *Ecole Polytechnique Fédérale de Lausanne (EPFL), Lausanne, Switzerland*
- ⁴¹ *Physik-Institut, Universität Zürich, Zürich, Switzerland*
- ⁴² *Nikhef National Institute for Subatomic Physics, Amsterdam, The Netherlands*
- ⁴³ *Nikhef National Institute for Subatomic Physics and VU University Amsterdam, Amsterdam, The Netherlands*
- ⁴⁴ *NSC Kharkiv Institute of Physics and Technology (NSC KIPT), Kharkiv, Ukraine*
- ⁴⁵ *Institute for Nuclear Research of the National Academy of Sciences (KINR), Kyiv, Ukraine*
- ⁴⁶ *University of Birmingham, Birmingham, United Kingdom*
- ⁴⁷ *H.H. Wills Physics Laboratory, University of Bristol, Bristol, United Kingdom*
- ⁴⁸ *Cavendish Laboratory, University of Cambridge, Cambridge, United Kingdom*
- ⁴⁹ *Department of Physics, University of Warwick, Coventry, United Kingdom*
- ⁵⁰ *STFC Rutherford Appleton Laboratory, Didcot, United Kingdom*
- ⁵¹ *School of Physics and Astronomy, University of Edinburgh, Edinburgh, United Kingdom*
- ⁵² *School of Physics and Astronomy, University of Glasgow, Glasgow, United Kingdom*
- ⁵³ *Oliver Lodge Laboratory, University of Liverpool, Liverpool, United Kingdom*
- ⁵⁴ *Imperial College London, London, United Kingdom*
- ⁵⁵ *School of Physics and Astronomy, University of Manchester, Manchester, United Kingdom*
- ⁵⁶ *Department of Physics, University of Oxford, Oxford, United Kingdom*
- ⁵⁷ *Massachusetts Institute of Technology, Cambridge, MA, United States*
- ⁵⁸ *University of Cincinnati, Cincinnati, OH, United States*
- ⁵⁹ *University of Maryland, College Park, MD, United States*
- ⁶⁰ *Syracuse University, Syracuse, NY, United States*
- ⁶¹ *Pontifícia Universidade Católica do Rio de Janeiro (PUC-Rio), Rio de Janeiro, Brazil, associated to ²*
- ⁶² *University of Chinese Academy of Sciences, Beijing, China, associated to ³*
- ⁶³ *Institute of Particle Physics, Central China Normal University, Wuhan, Hubei, China, associated to ³*
- ⁶⁴ *Departamento de Física, Universidad Nacional de Colombia, Bogota, Colombia, associated to ⁸*
- ⁶⁵ *Institut für Physik, Universität Rostock, Rostock, Germany, associated to ¹²*
- ⁶⁶ *National Research Centre Kurchatov Institute, Moscow, Russia, associated to ³²*
- ⁶⁷ *Yandex School of Data Analysis, Moscow, Russia, associated to ³²*
- ⁶⁸ *Instituto de Física Corpuscular (IFIC), Universitat de Valencia-CSIC, Valencia, Spain, associated to ³⁷*
- ⁶⁹ *Van Swinderen Institute, University of Groningen, Groningen, The Netherlands, associated to ⁴²*

^a *Universidade Federal do Triângulo Mineiro (UFTM), Uberaba-MG, Brazil*

^b *Laboratoire Leprince-Ringuet, Palaiseau, France*

^c *P.N. Lebedev Physical Institute, Russian Academy of Science (LPI RAS), Moscow, Russia*

^d *Università di Bari, Bari, Italy*

^e *Università di Bologna, Bologna, Italy*

^f *Università di Cagliari, Cagliari, Italy*

^g *Università di Ferrara, Ferrara, Italy*

^h *Università di Genova, Genova, Italy*

ⁱ *Università di Milano Bicocca, Milano, Italy*

^j *Università di Roma Tor Vergata, Roma, Italy*

^k *Università di Roma La Sapienza, Roma, Italy*

^l *AGH - University of Science and Technology, Faculty of Computer Science, Electronics and Telecommunications, Kraków, Poland*

^m *LIFAEELS, La Salle, Universitat Ramon Llull, Barcelona, Spain*

ⁿ *Hanoi University of Science, Hanoi, Viet Nam*

^o *Università di Padova, Padova, Italy*

^p *Università di Pisa, Pisa, Italy*

^q *Università degli Studi di Milano, Milano, Italy*

^r *Università di Urbino, Urbino, Italy*

^s *Università della Basilicata, Potenza, Italy*

^t *Scuola Normale Superiore, Pisa, Italy*

^u *Università di Modena e Reggio Emilia, Modena, Italy*